Probing Multi-Strange Dibaryon with Proton-Omega Correlation in High-energy Heavy Ion Collisions

Kenji Morita,[1, *] Akira Ohnishi,[1, †] Faisal Etminan,[2, ‡] and Tetsuo Hatsuda[3, §]

[1]*Yukawa Institute for Theoretical Physics, Kyoto University, Kyoto 606-8502, Japan*
[2]*Department of Physics, Faculty of Sciences, University of Birjand, Birjand 97175-615, Iran*
[3]*Theoretical Research Division, Nishina Center, RIKEN, Saitama 351-0198, Japan*
iTHES Research Group, RIKEN, Saitama 351-0198, Japan
(Dated: May 24, 2016)

Two-particle intensity correlation between the proton (p) and the Omega-baryon (Ω) in high-energy heavy ion collisions is studied to unravel the possible spin-2 $p\Omega$ dibaryon recently suggested by lattice QCD simulations. The ratio of correlation functions between small and large collision systems, $C_{\mathrm{SL}}(Q)$, is proposed to be a new measure to extract the strong $p\Omega$ interaction without much contamination from the Coulomb attraction. Relevance of this quantity to the experimental observables in heavy-ion collisions is also discussed.

PACS numbers: 25.75.Gz, 21.30.Fe, 13.75.Ev

Introduction.— The baryon-baryon interactions serve as crucial inputs for understanding possible dibaryons with strangeness (S). In particular, the spin-0 H state with $S = -2$ [1] and the spin-2 nucleon-Omega ($N\Omega$) state with $S = -3$ [2] are among the most promising candidates for bound or resonant dibaryons, since the Pauli exclusion principle does not operate among quarks in these channels [3, 4]. Indeed, it was recently reported from first-principles lattice QCD simulations with heavy quark masses that there exist sizable attractions in the spin-0 H channel [5, 6] and in the spin-2 $N\Omega$ channel [7], although the quantitative answers would be obtained only by the on-going physical point simulations [8].

Experimentally, high-energy heavy ion collisions at the Relativistic Heavy-Ion Collider (RHIC) and the Large Hadron Collider (LHC) provide unique opportunities for multi-strange dibaryons [9]. For example, the search for the H-dibaryon has been conducted both at RHIC [10] and LHC [11]. More generally, the final state interactions for identical and non-identical hadrons after freeze-out [12, 13] have been shown to be sensitive to the low-energy scattering parameters [10, 14–17].

In this Letter, motivated by the recent study on the $N\Omega$ interaction in lattice QCD [7], we study the proton(p)-Ω correlation function in the relativistic heavy ion collisions to probe the nature of the $S = -3$ dibaryon. We propose that the ratio of the $p\Omega$ correlation functions with different source sizes is a good measure to extract the strong interaction between p and Ω without much contamination from the Coulomb attraction.

$N\Omega$ interaction.— In the S-wave $N\Omega$ system, there exist two possible channels, ${}^5S_2$ and ${}^3S_1$, where ${}^{2s+1}L_J$ denotes the state with spin-s, L-wave, and total angular momentum J. As long as the strong interaction is concerned, the lowest threshold in octet-decuplet and decuplet-decuplet channels is $N\Omega$ at 2610MeV. In the octet-octet channel, $\Lambda\Xi$ (with the threshold at 2430MeV) and $\Sigma\Xi$ (at 2507MeV) lie below $N\Omega$. For ${}^5S_2$, the cou-

pling of $N\Omega$ to these octet-octet channels occurs only through the D-wave, and thus it is dynamically suppressed. On the other hand, for ${}^3S_1$, the sizable coupling to octet-octet channels through the rearrangement of quarks is expected in the S-wave.

Let us first consider the $N\Omega$ interaction in the ${}^5S_2$ channel where recent lattice QCD simulations with heavy quarks (m_π=875 MeV and m_K=916 MeV) show attraction for all range of their relative distance r [7]. In Fig. 1, the lattice data are shown by black circles with statistical error bars. The data can be fitted well by an attractive Gaussian core + an attractive (Yukawa)^2 tail with a form factor; $V(r) = b_1 e^{-b_2 r^2} + b_3(1 - e^{-b_4 r^2})(e^{-b_5 r}/r)^2$, where $b_{1,3} < 0$ and $b_{2,4,5} > 0$. The best fit is shown by the red solid line in the figure denoted by V_{II}. Assuming that the qualitative form of this attractive potential does not change even for physical quark masses, we generate a series of potentials by varying the range-parameter at long distance, b_5. Two typical examples are V_{I} with weaker attraction and V_{III} with stronger attraction in Fig. 1. By solving the Schrödinger equation using these potentials with the physical baryon masses, one finds no bound state for V_{I}, a shallow bound state for V_{II}, and a deep bound state for V_{III}. The binding energies, the scattering lengths [26] and the effective ranges in the ${}^5S_2$ $p\Omega$ channel with and without the Coulomb potential are summarized in Table I.

As for the $N\Omega$ interaction in the ${}^3S_1$ channel, there would be a strong coupling to the octet-octet channels when the spatial distance between N and Ω becomes small. We model this by complete absorption of the $N\Omega$ wave function at short distance $r < r_0$. We choose $r_0 = 2$ fm, because the Coulomb potential dominates over $V_{\mathrm{I,II,III}}$ for $r > 2$ fm.

$N\Omega$ Correlation function.— The pairwise hadronic interaction gives enhancement or reduction of the observed number of pairs with small relative momenta in heavy ion collisions. In particular, the correlation function of
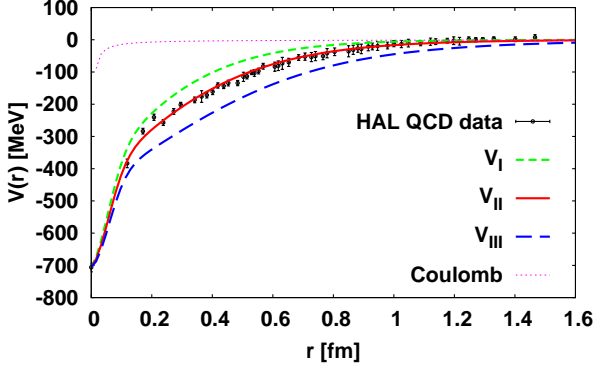
FIG. 1: Three typical examples of the $N\Omega$ potential. The black circles with error bars stand for the lattice QCD data with heavy quark masses [7]. The red line ($V_{\rm II}$) corresponds to a fit to the lattice data with a Gaussian + (Yukawa)^2 form. The green short-dashed line ($V_{\rm II}$) and the blue long-dashed line ($V_{\rm III}$) denote the potentials with weaker and stronger attractions, respectively. The Coulomb potential for the $p\Omega$ system is also shown by the purple dashed line.

TABLE I: The binding energy ($E_{\rm B}$), the scattering length (a_0) and the effective range ($r_{\rm eff}$) with and without the Coulomb attraction in the $p\Omega$ system. Physical masses of the proton and Ω are used.

Spin-2 $N\Omega$ Potentials		$V_{\rm I}$	$V_{\rm II}$	$V_{\rm III}$
without Coulomb	$E_{\rm B}$ [MeV]	$-$	0.05	24.8
	a_0 [fm]	-1.0	23.1	1.60
	$r_{\rm eff}$ [fm]	1.15	0.95	0.65
with Coulomb	$E_{\rm B}$ [MeV]	$-$	6.3	26.9
	a_0 [fm]	-1.12	5.79	1.29
	$r_{\rm eff}$ [fm]	1.16	0.96	0.65

non-identical pairs is directly related to the pairwise interaction due to the absence of the quantum statistical effect [13]. The $p\Omega$ correlation function is given in terms of the two-particle distribution $N_{p\Omega}(\boldsymbol{k}_p, \boldsymbol{k}_\Omega)$ normalized by the product of the single particle distributions, $N_\Omega(\boldsymbol{k}_\Omega)N_p(\boldsymbol{k}_p)$, with $\int_{x_i} \equiv \int d^4 x_i$,

$$C(\boldsymbol{Q}, \boldsymbol{K}) = \frac{N_{p\Omega}(\boldsymbol{k}_p, \boldsymbol{k}_\Omega)}{N_p(\boldsymbol{k}_p)N_\Omega(\boldsymbol{k}_\Omega)} \quad (1)$$
$$\simeq \frac{\int_{x_p}\int_{x_\Omega} S_p(x_p, \boldsymbol{k}_p)S_\Omega(x_\Omega, \boldsymbol{k}_\Omega)\,|\Psi_{p\Omega}(\boldsymbol{r}')|^2}{\int_{x_p} S_p(x_p, \boldsymbol{k}_p)\int_{x_\Omega} S_\Omega(x_\Omega, \boldsymbol{k}_\Omega)},$$

where relative and total momenta are defined as $\boldsymbol{Q} = (m_p\boldsymbol{k}_\Omega - m_\Omega\boldsymbol{k}_p)/M$ and $\boldsymbol{K} = \boldsymbol{k}_p + \boldsymbol{k}_\Omega$, respectively, with $M \equiv m_p + m_\Omega$. The source functions $S_i(x_i, \boldsymbol{k}_i) \equiv E_i\frac{dN_i}{d^3\boldsymbol{k}_i d^4 x_i}$, with $i = p, \Omega$ and $E_i = \sqrt{\boldsymbol{k}_i^2 + m_i^2}$, denote the phase space distribution of p and Ω at freeze-out. The final state interaction after the freeze-out is described by the two-particle wave function $\Psi_{p\Omega}$, in which the shift of the relative coordinate $\boldsymbol{r} = \boldsymbol{x}_\Omega - \boldsymbol{x}_p$ to $\boldsymbol{r}' = \boldsymbol{r} - \boldsymbol{K}(t_p - t_\Omega)/M$ accounts for the possible difference in the emission time between p and Ω. In the following, we assume that the pair purity is unity; i.e. the weak decay contribution to p can be removed experimentally and that to Ω is negligible [10, 18].

Taking into account the spin degeneracy, we have $|\Psi_{p\Omega}|^2 = \frac{5}{8}|\Psi_5(\boldsymbol{r})|^2 + \frac{3}{8}|\Psi_3(\boldsymbol{r})|^2$, where Ψ_5 (Ψ_3) denotes the wave functions in spin-2 (spin-1) channel. The strong interaction is short ranged and modifies only the S-wave component of the wave function, so that we may write

$$\Psi_{5(3)}(\boldsymbol{r}) = [\psi^C(\boldsymbol{r}) - \psi_0^C(r)] + \chi_{\rm sc(abs)}(r). \quad (2)$$

Here $\psi^C(\boldsymbol{r})$ is the Coulomb wave function characterized

by the reduced mass $\mu = 601$ MeV and the Bohr radius $a = (\mu\alpha)^{-1} \simeq 45$ fm of the $p\Omega$ system. Its S-wave component is denoted by $\psi_0^C(r)$. The scattering wave function in the ${}^5S_2$ state, $\chi_{\rm sc}(r)$, is obtained by solving the Schrödinger equation with both the strong interaction ($V_{\rm I,II,III}$) and the Coulomb interaction. Note that $\chi_{\rm sc}(r)$ reduces to $\psi_0^C(r)$ in the absence of strong interaction. On the other hand, the wave function $\chi_{\rm abs}(r)$ in the ${}^3S_1$ channel is zero for $r \leq r_0$ due to the strong absorption into octet-octet states, while it is identical to the Coulomb wave function for $r > r_0$:

$$\chi_{\rm abs}(r) = \theta(r - r_0)\frac{1}{2i\bar{r}}\left(H_0^+(\bar{r}) - F(\bar{r}_0)H_0^-(\bar{r})\right). \quad (3)$$

Here $Q = |\boldsymbol{Q}|$, $\bar{r} = Qr$, $\bar{r}_0 = Qr_0$, and $H_{L=0}^+$ ($H_{L=0}^-$) is the outgoing (incoming) Coulomb function which reduces to $e^{+i\bar{r}}$ ($e^{-i\bar{r}}$) without the Coulomb force [19]. Note that $F(\bar{r}_0) = H_0^+(\bar{r}_0)/H_0^-(\bar{r}_0)$, so that $\chi_{\rm abs}(r)$ is continuous across $r = r_0$. In the absence of the absorption, we have $\chi_{\rm abs}(r)|_{r_0\to 0} = \psi_0^C(r)$, since $F(\bar{r}_0 = 0) = 1$.

Case with static source.— We now consider the following static source function with spherical symmetry to extract the essential part of physics;

$$S_i(x_i, \boldsymbol{k}_i) = \mathcal{N}_i E_i\, e^{-\frac{\boldsymbol{x}_i^2}{2R_i^2}}\,\delta(t - t_i), \quad (i = p, \Omega). \quad (4)$$

Here R_i is a source size parameter, while $\mathcal{N}_i$ is a normalization factor which cancels out between the numerator and denominator together with E_i in Eq.(1). Assuming the equal-time emission $t_p = t_\Omega$ for the moment, one obtains a concise formula,

$$C(Q) = \int [dr]\int \frac{d\Omega}{4\pi}|\psi^C(\boldsymbol{r})|^2$$
$$+ \frac{5}{8}\int [dr]\{|\chi_{\rm sc}(r)|^2 - |\psi_0^C(r)|^2\}$$
$$+ \frac{3}{8}\int [dr]\{|\chi_{\rm abs}(r)|^2 - |\psi_0^C(r)|^2\}, \quad (5)$$

where $[dr] = \frac{1}{2\sqrt{\pi}R^3}dr\,r^2 e^{-\frac{r^2}{4R^2}}$ with $R = \sqrt{(R_p^2 + R_\Omega^2)/2}$ being the effective size parameter. $\int d\Omega$ is the integration over the solid angle between $\boldsymbol{Q}$ and $\boldsymbol{r}$. Without

the Coulomb interaction, the integration of the first line in Eq.(5) simply gives unity. The second (third) line is nothing but a spatial average of the difference between the S-wave probability density with and without the strong interaction, where the source function acts as a weight factor. Similar formula for the $\Lambda\Lambda$ correlation has been previously derived with the quantum statistical effect [16].

Let us now discuss the effects of the elastic scattering in the $^5S_2$ channel, the strong absorption in the $^3S_1$ channel and the long range Coulomb interaction, step by step on the basis of Eq.(5). First, we neglect the Coulomb interaction, so that the first line of Eq. (5) is unity and $\psi_0^C(r)$ becomes the free spherical wave $j_0(\bar{r})$. For a weak attraction without bound state (V_I), the probability density $|\chi_{sc}(r)|^2$ in the $^5S_2$ channel is slightly enhanced from the free one at short distances and at small Q. This leads to $C(Q)$ represented by the green solid curve in Fig. 2(a) illustrated for a characteristic source size $R_p = R_\Omega = 2.5$ fm measured in the pp correlation for mid-central events [14, 15]. As the attraction increases towards and across the unitary limit where the scattering length diverges, the enhancement of $C(Q)$ becomes prominent as represented by the red solid curve corresponding to V_{II} in Fig. 2(a). As the attraction becomes even stronger, $\chi_{sc}(r)$ for small Q starts to oscillate and to be suppressed inside the source radius R due to large local momentum $q(r) = \sqrt{2\mu(E-V)}$. This effect tames the enhancement of $C(Q)$ and eventually leads to a suppression of $C(Q)$ as represented by the blue solid curve corresponding to V_{III} in Fig. 2(a).

In the $^3S_1$ channel, the probability density $|\chi_{abs}(r)|^2$ is zero at short distances. This implies that the absorption effect tends to suppress the particle correlation as indicated by the third line Eq. (5). The dashed lines in Fig. 2(a) show $C(Q)$ with both the $^5S_2$ scattering and the $^3S_1$ absorption: The absorption effect is not negligibly small, but is not significantly large to change the qualitative behavior of $C(Q)$ obtained by the $^5S_2$ scattering alone.

Shown in Fig. 2(b) is $C(Q)$ without the Coulomb interaction for three typical momenta ($Q = 20, 40$, and 60 MeV) as a function of a_0^{-1}. By shifting the parameter b_5 in the $N\Omega$ potential, one can change the scattering length a_0 from negative to positive values without substantial change of the effective range r_{eff}: The arrows in the figure indicate a_0^{-1} corresponding to $V_{I,II,III}$. For weak (strong) attraction where $a_0^{-1} < 0$ ($a_0^{-1} > 0$), $C(Q)$ is enhanced (suppressed) from unity, while it is substantially enhanced around the unitary limit $a_0^{-1} = 0$. This implies that $C(Q)$ for certain range of Q would provide a useful measure to identify the strength of the $N\Omega$ attraction.

Once we include the Coulomb interaction between the positively charged p and the negatively charged Ω, an strong enhancement of $C(Q)$ at small Q is introduced by
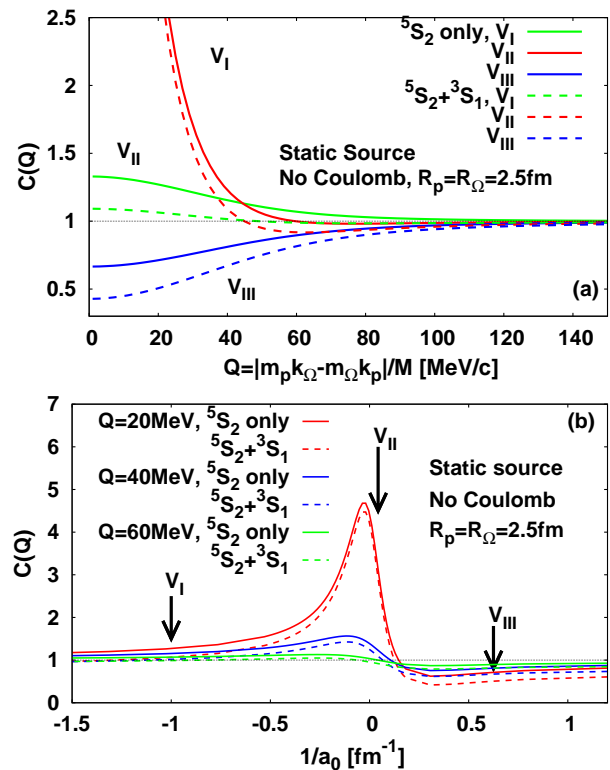

FIG. 2: $p\Omega$ correlation function for the static source with $R_p = R_\Omega = 2.5$ fm. The Coulomb interaction is switched off. (a) Solid (dashed) lines denote the correlations with only the $^5S_2$ scattering (with both the $^5S_2$ scattering and the $^3S_1$ absorption). (b) $C(Q)$ for $Q = 20, 40$ and 60 MeV as a function of a_0^{-1} obtained by changing the attraction of the $N\Omega$ potential through the parameter b_5.

the long-range attraction. The results with the Coulomb attraction are shown by the solid lines in Fig. 3(a) for $R_{p,\Omega} = 2.5$ fm. The ordering of the correlations with respect to the strength of the strong interaction is less visible at small Q due to the Coulomb enhancement. Nevertheless. the difference can still be seen for intermediate values of Q. The dashed lines in Fig. 3(a) represent $C(Q)$ for larger source size, $R_{p,\Omega} = 5$ fm. In this case, the correlation function is more sensitive to the long-range part of the interaction as found for proton-proton correlation [12, 13].

Shown in Figure 3(b) is a small-large (SL) ratio of the correlation functions defined by $C_{SL}(Q) \equiv C_{R_{p,\Omega}=2.5fm}(Q)/C_{R_{p,\Omega}=5fm}(Q)$. An advantage of this ratio is that the effect of the Coulomb interaction for small Q is largely cancelled, so that it has a good sensitivity to the strong interaction without much contamination from the Coulomb interaction.

Effects of expansion and freeze-out time.— The results so far have been obtained with a simplified static source function (4). In reality, the collective expansion takes place in high energy heavy ion collisions. Also, the freeze-out of multi-strange hadrons may occur prior to
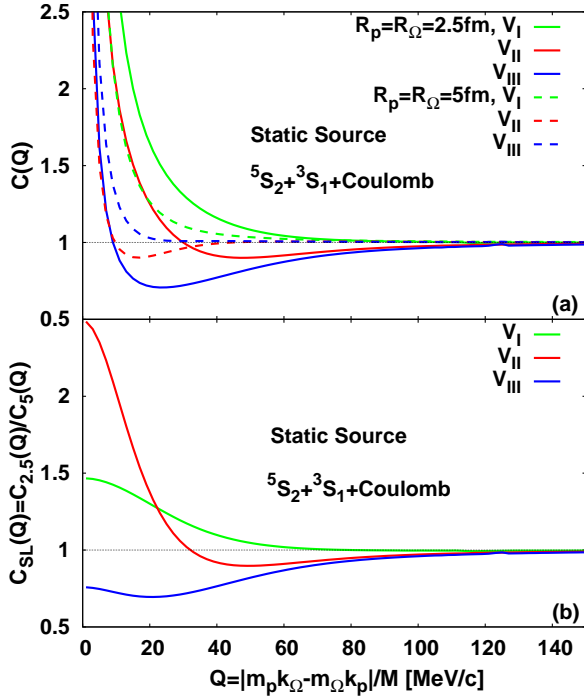
FIG. 3: (a) The correlation function with both strong and the Coulomb attractions for two different values of the static source sizes, $R_{p,\Omega} = 2.5$ fm (solid lines) and 5 fm (dashed lines). (b) The small-large ratio $C_{SL}(Q)$ for the static source between the different source sizes, $R_{p,\Omega} = 2.5$ and 5 fm.
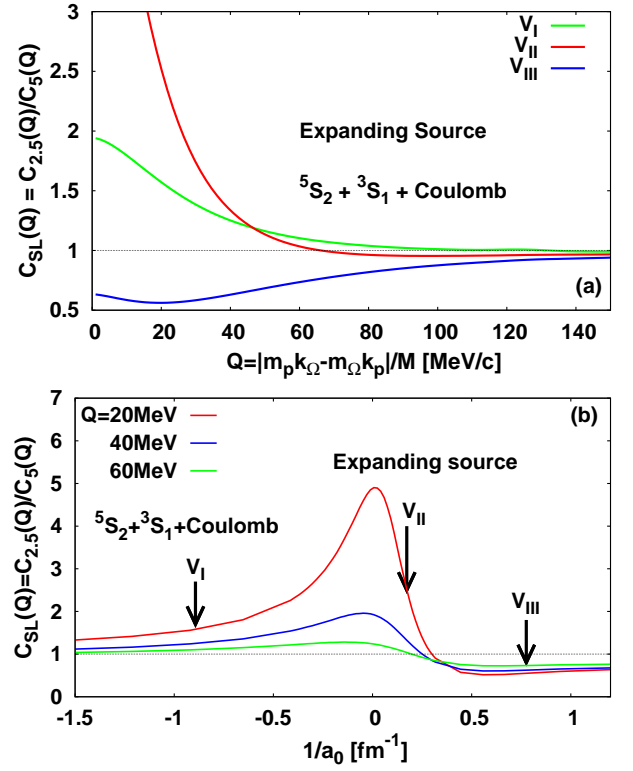

FIG. 4: (a) The small-large ratio $C_{SL}(Q)$ as a function of Q for three typical potentials. (b) The same ratio as (a) as a function of a_0^{-1}. In both figures, both the strong and Coulomb interactions are included.

other hadrons due to small cross sections [21, 22]. To see the influences of these dynamical properties, we consider the following source model with 1-dim Bjorken expansion [20],

$$S(x_i, \boldsymbol{k}_i) = \mathcal{N}'_i E_i^{\mathrm{tr}} \frac{1}{e^{E_i^{\mathrm{tr}}/T_i} + 1} e^{-\frac{x^2+y^2}{2(R_i^{\mathrm{tr}})^2}} \delta(\tau - \tau_i), \quad (6)$$

where $E_i^{\mathrm{tr}} = \sqrt{(\boldsymbol{k}_i^{\mathrm{tr}})^2 + m_i^2} \cosh(y_i - \eta_s)$ with the momentum rapidity y_i and the space-time rapidity $\eta_s = \ln \sqrt{(t+z)/(t-z)}$. The temperature and the proper-time at the thermal freeze-out are denoted by T_i and τ_i, respectively. The transverse source size is denoted by R_i^{tr}. We consider a small system with $R_p^{\mathrm{tr}} = R_\Omega^{\mathrm{tr}} = 2.5$ fm and a large system with $R_p^{\mathrm{tr}} = R_\Omega^{\mathrm{tr}} = 5$ fm. Following the results of the dynamical analyses of the peripheral and central Pb+Pb collisions at $\sqrt{s_{NN}} = 2.76$ TeV with hydrodynamics + hadronic transport [21], we take τ_p (τ_Ω) = 3 (2) fm for the former, and τ_p (τ_Ω) = 20 (10) fm for the latter as characteristic values. We take $T_{p,\Omega}$ =164 MeV for peripheral collisions [23], while $T_p(T_\Omega)$=120 (164) MeV for central collisions [24]. Under the expanding source, Eq.(1) has explicit $\boldsymbol{K}$ dependence: For illustrative purpose, we take the total longitudinal momentum to be zero $K_z = 0$ and the total transverse momentum to be $|\boldsymbol{K}^{\mathrm{tr}}|$=2.0 (2.5) GeV for peripheral (central) collisions which correspond to the twice of mean $|\boldsymbol{k}_p^{\mathrm{tr}}|$ values of the

proton [25].

Figure 4(a) demonstrates the effect of the dynamical property on $C_{SL}(Q)$: Its comparison to Fig.3(b) for the static source indicates no significant difference as far as the ratio $C_{SL}(Q)$ is concerned. Figure 4(b) shows $C_{SL}(Q)$ as a function of a_0^{-1}: Its comparison to Fig.2(b) on $C(Q)$ implies that the effect of the Coulomb interaction is nicely cancelled in the small-large ratio, so that the strong $N\Omega$ interaction can be constrained by the measurements of this ratio. Moreover, taking the ratio of $C(Q)$ reduces the apparent reduction of its sensitivity to the strong interaction due to the purity factor. There are in principle two ways to extract $C_{SL}(Q)$ experimentally in ultrarelativistic heavy ion collisions at RHIC and LHC: (i) Comparison of the peripheral and central collisions for the same nuclear system, and (ii) comparison of the central collisions with different system sizes, e.g. central Cu+Cu collisions and central Au+Au collisions at RHIC.

Conclusion.— Motivated by the strong attraction at short distance between the proton and the Ω-baryon in the spin-2 channel suggested by the recent lattice QCD simulations, we studied the intensity correlation of the $p\Omega$ emission from relativistic heavy ion collisions. Not only the elastic scattering in the spin-2 channel, but also the strong absorption in the spin-1 channel and the long-

range Coulomb attraction are taken into account in our analysis. Depending on the strength of the $p\Omega$ attraction, the correlation function at small relative momentum changes substantially near the unitary limit. We have proposed that the ratio of the correlation function between the small and large collision systems, $C_{\mathrm{SL}}(Q)$, is insensitive to the Coulomb interaction and also to the source model of the emission. Thus it provides a useful measure to extract the strong interaction part of the $p\Omega$ attraction from the experiments at RHIC and LHC.

* Electronic address: kmorita@yukawa.kyoto-u.ac.jp
† Electronic address: ohnishi@yukawa.kyoto-u.ac.jp
‡ Electronic address: fetminan@birjand.ac.ir
§ Electronic address: thatsuda@riken.jp

[1] R. L. Jaffe, Phys. Rev. Lett. **38**, 195 (1977).
[2] T. Goldman, K. Maltman, J. G. J. Stephenson, K. E. Schmidt, and F. Wang, Phys. Rev. Lett. **59**, 627 (1987).
[3] M. Oka, Phys. Rev. D **38**, 298 (1988).
[4] A. Gal, Acta Phys. Polon. B **47**, 471 (2016) [arXiv:1511.06605 [nucl-th]].
[5] T. Inoue *et al.* [HAL QCD Collaboration], Prog. Theor. Phys. **124**, 591 (2010) [arXiv:1007.3559 [hep-lat]]; Phys. Rev. Lett. **106**, 162002 (2011) [arXiv:1012.5928 [hep-lat]]; Nucl. Phys. A **881**, 28 (2012) [arXiv:1112.5926 [hep-lat]].
[6] S. R. Beane *et al.* [NPLQCD Collaboration], Phys. Rev. Lett. **106**, 162001 (2011) [arXiv:1012.3812 [hep-lat]].
[7] F. Etminan *et al.* [HAL QCD Collaboration], Nucl. Phys. A **928**, 89 (2014) [arXiv:1403.7284 [hep-lat]].
[8] T. Doi *et al.* [HAL QCD Collaboration], arXiv:1512.01610 [hep-lat]; arXiv:1512.04199 [hep-lat].
[9] S. Cho *et al.* [ExHIC Collaboration], Phys. Rev. Lett. **106**, 212001 (2011) [arXiv:1011.0852 [nucl-th]]; Phys. Rev. C **84**, 064910 (2011) [arXiv:1107.1302 [nucl-th]].
[10] L. Adamczyk et al. [STAR Collaboration], Phys. Rev. Lett. **114**, 022301 (2015).
[11] J. Adam et al. [ALICE Collaboration], Phys. Lett. B **752**, 267 (2016).
[12] R. Lednicky and V. L. Lyuboshits, Sov. J. Nucl. Phys. **35**, 770 (1982), [Yad. Fiz. **35**, 1316 (1981)].
[13] See the reviews, W. Bauer, C. K. Gelbke and S. Pratt, Ann. Rev. Nucl. Part. Sci. **42**, 77 (1992). M. A. Lisa, S. Pratt, R. Soltz and U. Wiedemann, Ann. Rev. Nucl. Part. Sci. **55**, 357 (2005) [nucl-ex/0505014].
[14] L. Adamczyk et al. [STAR Collaboration], Nature **527**, 345 (2015).
[15] J. Adam *et al.* [ALICE Collaboration], Phys. Rev. C **92**, no. 5, 054908 (2015) [arXiv:1506.07884 [nucl-ex]].
[16] K. Morita, T. Furumoto and A. Ohnishi, Phys. Rev. C **91**, no. 2, 024916 (2015) [arXiv:1408.6682 [nucl-th]].
[17] A. Ohnishi, K. Morita, K. Miyahara and T. Hyodo, arXiv:1603.05761 [nucl-th].
[18] G. Agakishiev *et al.* [STAR Collaboration], Phys. Rev. Lett. **108**, 072301 (2012).
[19] M. Abramowitz and I. A. Stegun, *Handbook of Mathematical Functions, With Formulas, Graphs, and Mathematical Tables*, (Dover, 1974).
[20] S. Chapman, P. Scotto and U. W. Heinz, Heavy Ion Phys. **1**, 1 (1995) [hep-ph/9409349].
[21] X. Zhu, F. Meng, H. Song, and Y. X. Liu, Phys. Rev. C **91**, 034904 (2015).
[22] S. Takeuchi, K. Murase, T. Hirano, P. Huovinen, and Y. Nara, Phys. Rev. C **92**, 044907 (2015).
[23] B. B. Abelev *et al.* [ALICE Collaboration], Phys. Lett. B **728**, 216 (2014) Erratum: [Phys. Lett. B **734**, 409 (2014)]
[24] C. Shen, U. Heinz, P. Huovinen and H. Song, Phys. Rev. C **84**, 044903 (2011) [arXiv:1105.3226 [nucl-th]].
[25] B. Abelev *et al.* [ALICE Collaboration], Phys. Rev. C **88**, 044910 (2013) [arXiv:1303.0737 [hep-ex]].
[26] We use the "nuclear physics convention" in which scattering phase shift δ at small momentum is given as $\delta = -ka_0$.